Insight into non-enzymatic browning of shelf-stable orange juice during storage: A fractionation and kinetic approach

Running title: Fractionation and kinetics to study non-enzymatic browning of orange juice

Huong Tran Thuy ***Pham***[a*], *Archana* ***Bista***[a], *Biniam* ***Kebede***[a, b], *Carolien* ***Buvé***[a], *Marc* ***Hendrickx***[a] *and Ann* ***Van Loey***[a**]

[a]*KU Leuven, Department of Microbial and Molecular Systems (M^2S), Laboratory of Food Technology, Kasteelpark Arenberg 22 box 2457, 3001 Heverlee, Belgium*

Current affiliation

[b]*University of Otago, Department of Food Science, Box 56, Dunedin 9054, New Zealand*

*Author to whom correspondence should be addressed **during submission process**

Telephone: +32 16 37 42 84

E-mail: tranthuyhuong.pham@kuleuven.be

Author to whom correspondence should be addressed **on post-publication

Telephone: +32 16 32 15 67

E-mail: ann.vanloey@kuleuven.be

This article has been accepted for publication and undergone full peer review but has not been through the copyediting, typesetting, pagination and proofreading process which may lead to differences between this version and the Version of Record. Please cite this article as doi: 10.1002/jsfa.10418

Abstract

BACKGROUND: Non-enzymatic browning (NEB) is the main quality defect of shelf-stable orange juice and other fruit juices during storage. Previous studies on NEB focused solely on the soluble fraction of orange juice, regardless of both soluble and insoluble fractions turning brown during extended storage. Up to date, clear evidence of the relative contribution of both fractions to NEB is lacking in literature. This study investigated the contribution of the soluble and insoluble fractions of orange juice, which were obtained by centrifugation and ethanol precipitation, towards NEB during storage. In addition, changes in different NEB related attributes (e.g., AA degradation, browning index (BI), etc.) were quantified and kinetically modeled.

RESULTS: Evaluation of color during storage showed that the orange juice and the soluble compound-containing fractions turned brown in contrast to the insoluble fractions. The soluble compound-containing fractions showed exactly the same browning behavior upon storage as the plain orange juice. Based on the kinetic parameters obtained, the degradation of AA, the hydrolysis of sucrose, the increase of glucose and fructose content, and the formation of furfural and 5-hydroxymethylfurfural during storage were similar for the plain orange juice and the soluble compound-containing fractions.

CONCLUSION: Considering studies on NEB, this work provided evidence that the soluble fraction of orange juice plays the major role in NEB unlike the insoluble fraction which seems to have no contribution. Furthermore, results from this work demonstrate the potential use of the soluble fraction as an orange juice based model system of reduced complexity in order to further investigate NEB processes.

Keywords

Non-enzymatic browning; orange juice; ascorbic acid degradation, soluble fractions, insoluble fractions; storage.

INTRODUCTION

Orange juice is a heterogeneous multiphase system consisting of serum, cloud, and pulp.[1,2] The serum is a clear aqueous fraction containing water soluble compounds such as vitamin C (ascorbic acid (AA) and dehydroascorbic acid (DHAA)), sugars, and organic acids, whereas the cloud and pulp are water insoluble fractions made of mainly polymers such as protein, pectin, cellulose, and hemicellulose.[2–5] Orange juice serum is a watery pale yellow liquid which has little perceivable juice aroma on its own and acts as the carrier solvent for the distributed cloud pulp.[3,6] Orange juice cloud is a suspension of particles ranging from 0.4 to 5 μm in size and is responsible for imparting the desirable texture, color, and flavor of orange juice along with the consumers expected turbidity.[5] Approximately 52% and 4.5% of the cloud is proteins and pectin, respectively, while the rest is made up of lipids, other cell wall polysaccharides and ash.[4,5,7] Orange juice pulp is composed of pieces of membrane materials from the ruptured juice sacs and segment walls.[3,5] As orange juice pulp contains large particles, it is commonly separated by centrifugation.[1–3] Meanwhile the polymers (proteins and polysaccharides) of orange juice cloud can be selectively precipitated by stepwise ethanol precipitation which is widely used for isolation and fractionation of plant cell wall polysaccharides.[2,8,9]

Color is one of the most important factors in the marketing of orange juice. Therefore, the detrimental changes in color of shelf-stable orange juice during storage, primarily caused by non-enzymatic browning (NEB) reactions, reduce consumer acceptance of the juice.[10–13] The NEB in pasteurized shelf-stable orange juice is hypothesized to be due to chemical reactions involving the degradation of some soluble compounds in the orange juice serum such as AA and sugars.[12,14–17] The degradation products (e.i., carbonyl compounds such as furfural) of these soluble compounds can polymerize with each other or react with amino acids to form brown colored compounds.[14,16,18–21] In addition, it is worth mentioning that sugar amine reactions of the classical Maillard type are of minor importance in citrus juice browning (including orange juice) because of the high acidity involved.[16] The quality defect caused by NEB is also known in other shelf-stable fruit juices (e.g., apple juice and strawberry juice) besides orange juice.[22–26]

It was observed that both the soluble (serum) and insoluble (pulp and cloud) fractions of thermally pasteurized shelf-stable orange juice turn brown upon storage.[9] Nonetheless, previous studies on NEB from literature focused solely on the role of AA, sugars, and amino acids present in the orange juice soluble fraction (serum),[12,17,20,27,28] whereas, no research focus was given to the role of insoluble compounds of orange juice cloud and pulp. Consequently, knowledge on the relative contribution of both fractions to NEB is lacking in literature.

Therefore, the aim of this study was twofold: (i) to fill the research gap in NEB of shelf-stable orange juice during storage by exploring the role of both soluble and insoluble fractions, and (ii) to kinetically model and compare the changes in different NEB related attributes of orange juice and different fractions derived thereof. For these purposes, plain orange juice was separated into different fractions using a stepwise approach based on centrifugation and ethanol precipitation. The plain orange juice and its derived fractions were pasteurized to achieve shelf-stable products, subsequently stored at an elevated temperature of 42 °C, and their browning behavior was compared. To the best of our knowledge, it is for the first time that the browning of orange juice and its fractions during storage was studied simultaneously and a quantitative comparison among different samples was made based on estimated kinetic parameters.

MATERIALS AND METHODS

Preparation of orange juice and different fractions

A single batch of freshly produced single strength refrigerated orange juice (12 carton boxes of 1 L) was purchased and stored for one day in a cooling room (4 °C) before the preparation of samples. The orange juice was not from concentrate juice. The preparation step was conducted as much as possible in a cooling room at 4 °C. Centrifugation and ethanol precipitation were applied to sequentially fractionate the orange juice into six different fractions (**Figure 1**): a supernatant, pellet, 20% and 70% ethanol soluble fractions (ES20 and ES70, respectively), and 20% and 70% ethanol precipitated fractions (EP20 and EP70, respectively). The precipitations at ethanol concentrations of 20 and 70% were selected as a previous work[9] showed a significant difference in the composition of the polymer fractions from orange juice cloud that precipitated at these two ethanol concentrations. More specific, the polymer fraction which was

precipitated at 20% ethanol was rich in proteins and arabinogalactans while the polymer fraction which was precipitated at 70% ethanol was mainly rich in pectin.[9]

At first, the orange juice was centrifuged (1000xg, 4 °C, and 15 min) (J2-HS centrifuge, Beckman, Brea, CA, U.S.A.) to separate the supernatant from the pellet which mainly contains water insoluble cell wall fragments (mainly orange juice pulp). The obtained pellet was washed with ultrapure water, recentrifuged (1000xg, 4 °C, and 15 min) and suspended in citric acid buffer (pH 3.8). Part of the supernatant fraction was further fractionated into ES20, ES70, EP20, and EP70 through stepwise ethanol precipitation. More specific, to part of the supernatant, absolute ethanol was added until an ethanol concentration of 20% (v/v) was reached and the solution was left for precipitation (20 – 24 h) at 4 °C. This solution was then centrifuged (10000xg, 4 °C, and 15 min) to obtain two fractions: 20% ethanol soluble supernatant and 20% ethanol precipitated pellet. Subsequently, the ethanol precipitated pellet was washed with 20% ethanol, centrifuged (10000xg, 4 °C, and 15 min), and then dissolved in citric acid buffer (pH 3.8) to yield a EP20 fraction which contains part of the orange juice cloud that is precipitated at 20% ethanol. Part of the 20% ethanol soluble supernatant was subjected to a further ethanol precipitation step in which the ethanol concentration was increased to 70% (v/v). The 70% ethanol soluble supernatant and 70% ethanol precipitated pellet were collected after a centrifugation step (10000xg, 4 °C, and 15 min). Similarly, the 70% ethanol precipitated pellet was washed and dissolved in citric acid buffer to yield a EP70 fraction. Ethanol in the 20% and 70% ethanol soluble supernatant was removed using a rotavapor (IKA® RV 10 rotary evaporator, Digital, IKA-Werke GmbH & Co) to yield ES20 and ES70 fractions, respectively. In summary, the orange juice, supernatant, ES20 and ES70 fractions contain almost similar concentration of the soluble compounds and different amount/composition of the insoluble compounds. Meanwhile, the pellet, EP20, and EP70 fraction contain only insoluble compounds from the orange juice.

Finally, the plain orange juice and its derived fractions (e.g., supernatant, pellet, ES20, ES70, EP20, and EP70) were filled in glass jars (100 mL volume, 95 mm height, and 45 mm diameter) up to a volume of 80 mL and kept at 4 °C in a cooling room prior to the thermal treatment.

Thermal treatment

The thermal treatment of the orange juice and its derived fractions was carried out in a static steriflow pilot plant retort (Barriquand, Paris, France). This step aimed to achieve shelf-stable products which can be stored at room temperature or elevated temperatures over an extended storage time. As pH of orange juice and all other fractions was around 3.80, a pasteurization value of $^{10\,°C}P_{90\,°C}$ (P_o) = 3 min was selected. All the samples filled in glass jars were loaded into the retort for pasteurization at a holding temperature of 90 °C. Temperature profiles in the retort and at the coldest point of the sample were recorded using type T-thermocouples (Ellab, Hillerød, Denmark). At the end of the pasteurization process, samples were cooled down to 20 °C and removed from the retort.

Storage of the pasteurized samples

All the pasteurized samples (plain orange juice and fractions) were stored at an elevated temperature of 42 °C for eight weeks in a temperature controlled incubator protected from light. It has previously been confirmed that storage of shelf-stable single strength orange juice at 42 °C only accelerates the NEB process without inducing new reaction pathways.[29]

Sampling was done prior to storage (i.e. immediately after the pasteurization step) and at seven different moments (1 and 4 day(s), 1, 2, 4, 6, and 8 week(s)) during storage. For each sampling moment, three glass jars were randomly taken from the incubator. The content was mixed and divided uniformly to smaller tubes which were frozen in liquid nitrogen and stored at -40 °C, except for the ES20 and ES70 samples which were stored at -80 °C. Prior to analysis, samples were thawed in a circulating water bath at 20 °C for a standardized time.

Browning index measurement

Browning index (BI) was determined according to a method previously reported.[9] A portion of 10 mL of sample was centrifuged (1000xg, 4 °C, and 15 min) (J2-HS centrifuge, Beckman, Brea, CA, U.S.A.). Subsequently, 5 mL of the obtained supernatant was mixed with 5 mL of 95% ethanol and the solution was placed in an ice bath for 15 min to accelerate flocculation of the finely suspended particles. Next, the sample was recentrifuged (1000xg, 4 °C, and 15 min) and the supernatant was filtered (0.45 μm,

hydrophilic). The absorbance of the filtered supernatant was measured at 420 nm using a spectrophotometer (Ultraspec 2100pro UV/Visible spectrophotometer, GE Healthcare, Uppsala, Sweden) with a cell path length of 1 cm.

Ascorbic acid and total vitamin C determination

Determination of vitamin C included both ascorbic acid (AA) and dehydroascorbic acid (DHAA) and was based on a method of Wibowo et al.[29] and described earlier by Pham et al.[9] A portion of sample was mixed with extraction buffer (1% (w/v) m-phosphoric acid with 0.5% (w/v) oxalic acid, pH 2.0) in a ratio of 1:3 and the mixture was centrifuged (24000xg, 4 °C, and 15 min) (J2-HS centrifuge, Beckman, Brea, CA, U.S.A.). The extraction was performed in triplicate for each sample. Subsequently, the pH of the obtained supernatant was adjusted to 3.5 using 1 M NaOH or 1 M HCl. To determine the AA content, phosphate buffer (20 mM NaH_2PO_4 + 1 mM Na_2EDTA, pH 3.5) was added to part of the pH adjusted supernatant in a ratio of 2:1 and the mixture was filtered through a 0.45 μm syringe filter (hydrophilic) (Chromafil A-45/25, Macherey-Nagel, Düren, Germany) prior to injection in the high-performance liquid chromatography (HPLC) system. The total vitamin C content (sum of AA and DHAA) was determined in the form of AA adding a reducing agent (TCEP 2.5 mM tris (2-carboxyl-ethyl) phosphine in phosphate buffer, pH 3.5) to the other part of the pH adjusted supernatant in a ratio of 2:1 to reduce the DHAA present in the sample to AA. The mixture was centrifuged (19900xg, 23 °C, and 15 min) (Microfuge 22R, Beckman Coulter) and filtered (0.45 μm, hydrophilic). The analysis was performed in a HPLC (Dionex, Sunnyvale, CA, U.S.A.) with an AD25 UV-vis detection set at 245 nm. A Prevail C18 column (250x4.6 mm, 5 μm particle size, Grace, Columbia, MD, U.S.A.) with a corresponding guard column was used for chromatographic separation. The separation was carried out at 25 °C using isocratic elution with 1 mM Na_2EDTA and 10 mM CH_3COONH_4 at 0.8 mL min^{-1}. The injection volume was 25 μL. A calibration curve with AA (99%, Acros Organics, Geel, Belgium) in extraction buffer was prepared for quantification.

Determination of the dissolved and headspace oxygen content

The dissolved and headspace oxygen content of all the samples was measured during storage using a noninvasive OxySense® 4000B system (OxySense, Las Vegas, NV, U.S.A.). The principle of the oxygen

measurement is described by Wibowo et al.[29] For each condition, three bottles were equipped with oxygen sensors (O_2xyDots®) prior to filling. The measurement of the dissolved and headspace oxygen content was performed five times at room temperature for each bottle. The samples after taking from the incubator (42 °C) were equilibrated at room temperature (25°C) for at least one hour before measuring the oxygen content. As this is a nondestructive measurement, the same bottles could be used for the measurement during the whole storage experiment.

Determination of the sugar content

Sugars were extracted according to the procedure of Vervoort et al.[30] with some modifications. 50 µL of each Carrez I (15% w/v $K_4[Fe(CN)_6]$) and Carrez II (30% w/v $ZnSO_4$) was added to 1 mL of the sample and the mixture was homogenized using a vortex. After resting for 30 min at room temperature, the sample was centrifuged (19900xg, 4 °C, and 15 min) (Microfuge 22R, Beckman Coulter). The obtained supernatant was filtered (0.45 µm, hydrophilic) and 2 µL of a 10 fold dilution of the filtrate was injected into the HPLC system. The extraction was done in triplicate for each sample. The analysis was performed in a HPLC (Agilent 1200 series, Santa Clara, CA, USA) with evaporative light scattering detection. A Prevail™ carbohydrate ES column (analytical column 250x4.6 mm, 5 µm particle size, Alltech, Grace, Deerfield, IL) with Prevail C18 guard cartridge (7.5×4.6 mm, 5 µm particle size, Alltech, Grace, Deerfield, U.S.A.) was used for chromatographic separation. The separation was carried out at 30 °C using isocratic elution with 75% (v/v) acetonitrile/water at 1 mL min^{-1}. Identification was performed by comparing the retention times with the sugar standards (fructose, glucose, and sucrose), while quantification was carried out using calibration curves of the standards.

Determination of the furfural and 5-hydroxymethylfurfural content

The extraction and chromatographic analysis of furfural and 5-hydroxymethylfurfural (HMF) was based on a method of Wibowo et al.[29] with some modifications. 500 µL each of Carrez I reagent and Carrez II reagent was added to 10 mL of the sample and the mixture was vortexed. After resting for 30 min at room temperature, the sample was centrifuged (24000xg, 4 °C, and 15 min) (J2-HS centrifuge, Beckman, Brea, CA, U.S.A.). 1 mL of the obtained supernatant was applied on a C18 SPE precolumn (Sep-PAK Water, Milford,

U.S.A.), preconditioned with 2 mL methanol and 5 mL 0.5% acetic acid. After washing the SPE column with 2 mL of ultrapure water, furfural and HMF were selectively eluted with 4.5 mL ethyl acetate, and dried with anhydrous sodium sulfate. The eluate was filtered (0.45 μm) and the volume was adjusted to 5 mL with ethyl acetate. The extraction was performed in triplicate. The separation and analysis were carried out in a HPLC (Agilent 1200 series, Santa Clare, CA, U.S.A.) with UV-vis detector. The chromatographic separation was performed using a Zorbax Eclipse XDB C18 column (150×4.6 mm, 5 μm particle size, Agilent technologies, Diegem, Belgium) coupled to a Prevail C18 guard cartridge at 25 °C. The mobile phase was a mixture of 5/95 (v/v) acetonitrile/water at 1 mL min^{-1} isocratic elution. Furfural was detected at 277 nm and HMF was detected at 285 nm. Identification was performed comparing the retention time with furfural and HMF standards, while quantification was done using calibration curves of the standards.

Kinetic modelling

The evolution of different attributes of interest during storage was quantitatively evaluated by kinetic modelling of the data. For each attribute, model performance of several kinetic models was evaluated by examining $R^2_{adjusted}$ (**Eq. 5**) and by visual inspection of the parity plot (estimated values versus measured values) and the residual plot. For each attribute, the best performing model was selected and kinetic parameters were estimated by (non)linear regression analysis using Statistical Analysis System (SAS) software (SAS 9.3, Cary, NC). Following kinetic models have been selected, namely zero order (**Eq. 1**), first order (**Eq. 2**), first order fractional conversion (**Eq. 3**), and logistic (**Eq. 4**) models. In these equations, X is the parameter value at storage time t (weeks), X_0 is the initial value before storage, X_∞ are plateau values which are stable as a function of time, k and k_{max} are the apparent reaction rate constants, and λ (weeks) is the duration of lag phase in the logistic model. In **Eq. 5**, DF_{tot} and DF_{error} are total degree of freedom and degree of freedom of error, respectively, and SS is the sum of squares. The selected models should be considered as empirical models and should not be mechanistically interpreted.

$$X = X_0 + kt \text{ (zero order model for formation)} \quad (1)$$

$$X = X_0 \exp(-kt) \text{ (first order model for degradation)} \quad (2)$$

$$X = X_\infty + (X_0 - X_\infty) \exp(-kt) \quad (3)$$

$$X = \frac{X_\infty}{1+exp\left[\frac{4k_{max}}{X_\infty}(\lambda\text{-}t)+2\right]} \quad (4)$$

$$R^2_{adjusted} = 1 - \left[\frac{(DF_{tot}-1)\left(1-\frac{SS_{model}}{SS_{total}}\right)}{DF_{error}}\right] \quad (5)$$

Statistical differences between the estimated parameters of different samples were evaluated using their 95% confidence intervals which was obtained from the ANOVA table as an output of SAS.

RESULTS AND DISCUSSION

Color changes: Qualitative observations

It was observed that the color of the orange juice and all the fractions visually changed during storage (**Figure 2**). More specifically, the color of the orange juice and the soluble compound-containing fractions, being the supernatant, ES20, and ES70 fraction, changed from yellow-orange to brown and the brown color intensity increased with storage time. In addition, the pattern of browning during storage was similar for all the aforementioned samples. This is probably because of the fact that they are all containing a similar concentration of suspected NEB precursors such as AA, sugars, and amino acids. On the other hand, the insoluble compound-containing fractions such as the pellet, EP20, and EP70 which contain only insoluble compounds of orange juice pulp and cloud, did not turn brown during the entire storage period. Instead, their color was gradually bleaching from yellow to white. The color change of these samples could probably be attributed to the degradation of carotenoids, and/or the precipitation of carotenoid-containing particles during storage. In addition, the absence of brown color formation in the insoluble compound-containing fractions (EP20, EP70, and pellet fractions) indicates that NEB reactions did not take place in these samples.

These qualitative observations on color changes provide a first strong indication that only the soluble compounds of orange juice play an important role in NEB while the insoluble compounds of orange juice cloud and pulp seem not to have any contribution regardless the fact that both the serum and insoluble phase (cloud and pulp) turn brown during extended storage of the plain orange juice. A possible hypothesis is that, during storage, the brown compounds formed in the orange juice serum may adsorb onto the

insoluble compounds such as arabinogalactan proteins and/or protein-pectin complexes of orange juice cloud and pulp.[9]

Browning development

In the present study, browning index (BI), which is the absorbance at 420 nm of soluble brown compounds in an ethanol extracted sample, was used as an indicator for the evaluation of browning development. This index has generally been used in literature to determine the browning in orange juice and other citrus juices.[9,11,15,16,31,32] After the pasteurization, the BI of the pellet, EP20, and EP70 fractions was zero which was maintained throughout the entire storage period (**Figure 3**). This confirms that no NEB happens in these samples as already concluded from the visual color observations.

On the other hand, the BI of the nonstored pasteurized orange juice, supernatant, ES20, and ES70 was around 0.1. This value of BI obtained for the pasteurized orange juice before storage was similar to the results reported by Bull et al.[33] for pasteurized Valencia orange juice and Cortés et al.[34] for pasteurized Navel orange juice. The initial BI value of 0.1 of the nonstored samples could be attributed to the brown compounds that have been produced from NEB reactions during thermal processing and other inherent components of the juice such as free carotenoids.

The change in BI of the orange juice, supernatant, ES20, and ES70 during 8 weeks storage at 42 °C is illustrated in **Figure 3**. The results showed that the BI increased for all samples during storage which is in accordance with the previous visual observation in which the intensity of brown color increased with storage time (**Figure 2**). One of the main reasons which could explain the increase in BI is the accumulation of brown colored compounds resulting from the degradation of AA and/or sugars through NEB reactions during storage. In addition, a similar trend in the evolution of BI which sharply increased at the beginning of storage with a further evolution towards a stable value at the end of storage was noticed for the orange juice and the other soluble compound-containing fractions. The similarity amongst these samples is probably attributed to the similar composition of suspected NEB precursors such as AA, sugars, and amino acids in those matrices.

The evolution of BI during storage was quantitatively evaluated by the kinetics of the data. For all the samples that turned brown, the increase in BI during storage could be best described by a first order fractional conversion model ($R^2_{adj} \geq 0.97$). Different from our study, other researchers used complex polynomial models to describe the browning of citrus juice based on changes in absorbance at 420 nm,[35,36] whereas, first order models were used to describe the browning development in orange juice and orange juice serum during thermal treatment.[31] In the present work, the first order fractional conversion model was used to estimate the rate constant (k) and final BI values for the orange juice and the soluble compound-containing fractions (**Table 1**). Although the estimated k value was slightly higher for the supernatant, ES20, and ES70 than for the orange juice, no statistically significant difference in this parameter could be observed. Regarding to the final BI reached in the samples, the ES70 fraction showed the highest estimated final BI value. However, similar to the estimated k values, the estimated final BI values were not significantly different among these samples. These results revealed that there was no statistical difference in the browning development during storage of the orange juice and the soluble compound-containing fractions.

Kinetic modeling of changes in non-enzymatic browning related attributes

It has been reported in the previous sections that the orange juice and the fractions (supernatant, ES20, and ES70) which contain soluble compounds turned brown with storage time while the fractions (pellet, EP20, and EP70) which contain only insoluble compounds did not. Therefore, further analyses on the NEB related attributes were performed only for the orange juice and the soluble compound-containing fractions. In addition, to gain quantitative insight into the changes in different NEB related attributes, kinetic modeling was applied on the experimental data and kinetic parameters were estimated. Furthermore, a comparison among the samples was made based on the estimated parameters for each attribute. Kinetic modeling of the changes in NEB related attributes during storage of orange juice such as ascorbic acid degradation has been widely studied in literature. However, to the best of our knowledge, no open literature can be found which studies the changes during storage of orange juice in comparison to its fractions on such a wide range of NEB related attributes.

Changes in ascorbic acid content during storage

Figure 4A shows the changes in AA content during storage at 42 °C of the orange juice, supernatant, ES20, and ES70. As can be seen from the figure, the AA content decreased sharply in the first week of storage at 42 °C for all the samples, especially the ES20 and ES70 fractions. After one week of storage, the AA content has decreased by 75, 86, 100 and 94% for the orange juice, supernatant, ES20 and ES70, respectively, and by the end of 4 weeks storage no AA was detected in none of the samples. The fast drop in AA content at the beginning of storage could be due to a rapid oxidation of AA via the aerobic pathway in the presence of a high oxygen content. This is in agreement with the results of other studies which showed a fast degradation of AA at the beginning of storage.[29,37,38]

The degradation of AA in all the samples was best fitted with first order models ($R^2_{adj} \geq 0.97$), which is in agreement with literature on AA degradation in citrus juices, other fruit juices, and model systems.[22,29,39–41] The estimated model parameters in **Table 1** show lower rate constants (k) of AA degradation for the orange juice and supernatant than the ES20 and ES70 fractions. This could be attributed to the protection of antioxidants (e.g., carotenoids) presented in the cloud and pulp of the plain orange juice.[41] In addition, a change in total vitamin C content (sum of AA and DHAA content) (results not shown) during storage of the aforementioned samples was also investigated in this research and similar trends as for the AA content were observed.

Evolution of dissolved and headspace oxygen content during storage

As it is known that AA degradation in fruit juices is greatly affected by oxygen,[22,27,42] oxygen content has been monitored throughout the whole storage period both in the juice (dissolved oxygen) as well as in the headspace. As in present study, glass jars have been used for storage, oxygen diffusion through the package did not take place.

Dissolved and headspace oxygen content were measured during storage for the orange juice, supernatant, ES20, and ES70 and their changes are illustrated in **Figures 4B** and **4C**, respectively. It is clear that, for all the samples, the dissolved and headspace oxygen content decreased quickly in the first two weeks and four weeks of storage, respectively, and afterwards remained relatively constant at a very low level until the end

of eight weeks storage. This rapid disappearance of oxygen at the beginning of storage is caused by the consumption through oxidative reactions, especially AA oxidation. Changes in oxygen content were in accordance to the changes in AA content which showed a high AA degradation in the initial stage of storage (**Figure 4A**). Other studies already reported a fast depletion of oxygen content at the beginning of storage and linked this to the aerobic AA degradation in stored orange juice[16,29,39] and lemon juice.[42]

First order fractional conversion models were used to adequately describe the evolution of dissolved oxygen ($R^2_{adj} \geq 0.87$) and headspace oxygen ($R^2_{adj} \geq 0.98$) during storage of the orange juice and its soluble compound-containing fractions. The model for oxygen consumption determined in this study is in agreement with other studies including fruit juices [22,24] and, most important, with the study of Wibowo et al.[29] involving orange juice stored at different temperatures (20 to 42 °C) in polyethylene terephthalate (PET) bottles. The estimated kinetic parameters for dissolved oxygen (**Table 1**) show no significant differences in neither the rate constant nor the final oxygen content for all the samples reflecting a similar change in dissolved oxygen content during storage of these samples.

For the changes in headspace oxygen, a significant difference in the rate constant (*k*) could be observed among the samples with the ES20 and ES70 fractions showing higher rate constants than that of the orange juice and supernatant. This higher headspace oxygen consumption rate in the ES20 and ES70 fraction corresponds to the higher AA degradation rates observed in these samples. The headspace oxygen can be consumed directly by the oxidation reactions of the components on the interface of the juice and the headspace or indirectly through diffusion from the headspace to the juice. As expected, for all samples, the rate of oxygen consumption was higher for the dissolved oxygen than the headspace oxygen while the final oxygen content was similar (**Table 1**).

A high correlation was obtained between ascorbic acid loss and dissolved oxygen ($r = 0.93$-0.97), or headspace oxygen ($r = 0.94$-0.99) consumption. Thus, the decrease in oxygen in the orange juice and other samples may be attributed to its consumption through AA oxidation. Therefore, the availability of oxygen favors the aerobic degradation of AA, and thereby the formation of reactive carbonyl compounds which may contribute to browning upon further reactions.

Changes in sugars during storage

Sugar decomposition under acidic conditions resulting in the formation of reactive intermediates like HMF and 3-deoxyglucosone, is another well documented NEB reaction in orange juice as well as in other citrus juices.[12,15,43] The changes in sucrose, glucose, and fructose during storage of the orange juice, supernatant, ES20, and ES70 are shown in **Figures 4D**, **4E**, and **4F**, respectively. The results show that, for all samples, there was a decrease in sucrose content and increase in glucose and fructose content. These observations are in agreement with other studies and are due to sucrose inversion to glucose and fructose under acidic conditions during storage.[9,16,29] After eight weeks of storage of the orange juice, sucrose decreased by approximately 0.068 ± 0.004 mol L^{-1} while glucose and fructose increased around 0.058 ± 0.008 mol L^{-1} and 0.066 ± 0.004 mol L^{-1}, respectively. Hence, the decrease in sucrose content was similar to the increase in glucose and fructose. This trend was also observed for the changes in sugars in the supernatant, ES20 and ES70. In addition, the total sugar content (sum of sucrose, glucose, and fructose) in plain orange juice was similar to that of the other fractions and it remained relatively constant during storage. As sugars in orange juice including glucose and fructose can undergo acid catalyzed degradation to form NEB intermediates such as HMF,[43] the increase in glucose and fructose is expected to be lower than the decrease in sucrose. However, there was no significant difference in the decrease of sucrose and increase of glucose and fructose in our study. The most plausible explanation is that only a small amount of glucose and fructose can be significant enough to accelerate the formation of NEB intermediates.

Kinetic studies showed that, for all the samples, the decrease in sucrose could be adequately fitted by a first order model ($R^2_{adj} \geq 0.98$). Different from our results, Wibowo et al.[29] have used second order models to describe the sucrose hydrolysis in orange juice packed in PET bottles during storage at room temperature (20 °C) and elevated temperatures (28 to 42 °C). Regarding the increase of glucose and fructose during storage, zero order models were used to appropriately fit their evolution ($R^2_{adj} \geq 0.97$ and $R^2_{adj} \geq 0.95$, respectively). Based on the estimated rate constants (**Table 1**), there was no significant difference in the changes of sucrose, glucose, and fructose among the orange juice, supernatant, and ES20 whereas the ES70 showed a slightly higher rate constant for the hydrolysis of sucrose to glucose and fructose compared to the others.

Changes in furfural and HMF

Furfural and HMF were not detected in none of the samples after the pasteurization step. However, they were formed during storage and their contents increased with storage time (**Figures 4G** and **4H**). This observation is in accordance with the results reported by Pham et al.[9] and Wibowo et al.[29] for the formation of furfural and HMF during storage of shelf-stable orange juice stored in PET bottles. The furfural contents reached after eight weeks storage at 42 °C in the orange juice, supernatant, ES20, and ES70 samples were 1.28 ± 0.01, 1.17 ± 0.06 , 0.91 ± 0.01, and 1.01 ± 0.01 mg L^{-1}, respectively. Compared to the furfural content, HMF contents in all the samples by the end of an eight week storage period were almost 10 times higher.

The observed increase in furfural content in the orange juice, supernatant, ES20, and ES70 was best described by a zero order model ($R^2_{adj} \geq 0.98$) (**Figure 4G**). Other researchers have also reported that the change in furfural content in citrus juice including orange juice fitted to a zero order kinetic model.[29,42] It can be concluded from the parameter estimates that there was no significant difference in the rate constant (k) between any of the investigated samples revealing a similar furfural formation behavior as function of storage time.

For the formation of HMF, a logistic model (**Eq. 4**) was used to adequately describe the experimental data for all the samples containing soluble compounds, including orange juice, supernatant, ES20, and ES70 ($R^2_{adj} \geq 0.99$) (**Figure 4H**). During the first weeks of storage, the formation of HMF seemed to have an induction phase, in which HMF concentrations remained zero or only slightly increased. After this lag phase, the HMF concentration increased as function of storage time. The ES20 sample had the shortest duration of lag phase (λ), the lowest rate constant (k_{max}), and lowest final HMF concentration (X_∞) when compared to the other samples, being the orange juice, supernatant, and ES70 (**Table 1**). Meanwhile, there was no significant difference in either the duration of the lag phase, rate change (k_{max}), or final concentration when comparing the formation of HMF in the orange juice with the supernatant and ES70. Another study on the accumulation of HMF in orange juice during storage used a zero order model to

adequately fit the change although a lag phase was also observed for HMF formation at the beginning of storage.[29]

It is commonly stated in literature that furfural and HMF are important intermediates in NEB reactions of orange juice during storage.[43–45] Thus the evolution of furfural and HMF during storage was expected to have a high correlation with the evolution of BI value. Nevertheless, it was interestingly observed from our results that there was a fast rise in BI at the beginning of storage and after four weeks of storage it slowly increased (**Figure 3**), whereas, furfural concentration continued going up in a linear trend (**Figure 4G**) and HMF concentration increased exponentially (**Figure 4H**). The discrepancy in the evolution of BI and furfural and HMF could be probably because other intermediates are also responsible for the browning of orange juice especially in the early stage of storage. In addition, furfural and HMF may not be the limiting factor in the reactions from which brown compounds are formed.

CONCLUSIONS

It is for the first time that the role of soluble (serum) and insoluble (pulp and cloud) fraction of orange juice on non-enzymatic browning (NEB) was investigated simultaneously. The results of this study showed that the soluble compounds present in the serum of orange juice play an important role in NEB during storage while the insoluble compounds present in orange juice cloud and pulp do not have any contribution. The brown color of the insoluble compounds in the stored plain orange juice is hypothesized to result from the adsorption of brown compounds formed in the orange juice serum during storage. Browning behavior of the plain orange juice during storage was similar to the other soluble fractions that contain almost all of its soluble compounds. This is logical since the main difference among those samples is the concentration and/or composition of the insoluble compounds which do not contribute to the browning during storage. Given the similar kinetic model parameters, the ES70 fraction could be used as an orange juice model system with reduced complexity for future NEB studies.

ACKNOWLEDGMENTS

Huong T. T. Pham is a doctoral researcher funded by the Interfaculty Council for Development Cooperation (IRO). This research was financially supported be the Research Foundation Flanders (FWO) [Project

G0C3718N]. At the moment of the experimental work, Carolien Buvé was a doctoral researcher funded by the Research Foundation Flanders (FWO) [Project G0A7615N] and Biniam Kebede was a postdoctoral researcher funded by the Research Foundation Flanders (FWO) (12K2216N).

CONFLICT OF INTEREST

The authors of the present work declare no conflict of interests.

REFERENCES

1 Ringblom U. The orange book. *Lund, Sweden Tetra Pak Process Syst* (2004).

2 Ting S V., Rouseff RL. *Citrus fruits and their products: analysis, technology*. Dekker, 1986.

3 Brat P, Rega B, Alter P, Reynes M, Brillouet JM. Distribution of volatile compounds in the pulp, cloud, and serum of freshly squeezed orange juice. *J Agric Food Chem* **51**: 3442–3447 (2003).

4 Klavons JA, Bennett RD, Vannier SH. Nature of the protein constituent of commercial orange juice cloud. *J Agric Food Chem* **39**: 1545–1548 (1991).

5 Klavons JA, Bennett RD, Vannier SH. Physical/Chemical Nature of Pectin Associated with Commercial Orange Juice Cloud. *J Food Sci* **59**: 399–401 (1994).

6 Berk Z. Morphology and chemical composition. In: *Citrus Fruit Processing*. 2016, pp 9–54.

7 Galant AL, Widmer WW, Luzio GA, Cameron RG. Characterization of molecular structural changes in pectin during juice cloud destabilization in frozen concentrated orange juice. *Food Hydrocoll* **41**: 10–18 (2014).

8 Bian J, Peng F, Peng P, Xu F, Sun R-C. Isolation and fractionation of hemicelluloses by graded ethanol precipitation from Caragana korshinskii. *Carbohydr Res* **345**: 802–809 (2010).

9 Pham HTT, Bazmawe M, Kebede B, Buvé C, Hendrickx ME, Van Loey AM. Changes in the Soluble and Insoluble Compounds of Shelf-Stable Orange Juice in Relation to Non-Enzymatic Browning during Storage. *J Agric Food Chem* **67**: 12854–12862 (2019).

10 Álvarez J, Pastoriza S, Alonso-Olalla R, Delgado-Andrade C, Rufián-Henares JA. Nutritional and

physicochemical characteristic of commercial Spanish citrus juices. *Food Chem* **164**: 396–405 (2014).

11 Klim M, Nagy S. An improved method to determine nonenzymic browning in citrus juices. *J Agric Food Chem* **36**: 1271–1274 (1988).

12 Paravisini L, Peterson DG. Mechanisms Non-Enzymatic Browning in Orange Juice During Storage. *Food Chem* **289**: 320–327 (2019).

13 Bacigalupi C, Lemaistre MH, Boutroy N, Bunel C, Peyron S, Guillard V *et al.* Changes in nutritional and sensory properties of orange juice packed in PET bottles: An experimental and modelling approach. *Food Chem* **141**: 3827–3836 (2013).

14 Bharate SS, Bharate SB. Non-enzymatic browning in citrus juice: chemical markers, their detection and ways to improve product quality. *J Food Sci Technol* **51**: 2271–2288 (2014).

15 Paravisini L, Peterson DG. Characterization of browning formation in orange juice during storage. In: *ACS Symposium Series*. 2016, pp 55–65.

16 Roig MG, Bello JF, Rivera ZS, Kennedy JF. Studies on the occurrence of non-enzymatic browning during storage of citrus juice. *Food Res Int* **32**: 609–619 (1999).

17 Shinoda Y, Murata M, Homma S, Komura H. Browning and Decomposed Products of Model Orange Juice. *Biosci Biotechnol Biochem* **68**: 529–536 (2004).

18 Clegg KM, Morton AD. Carbonyl compounds and the non-enzymic browning of lemon juice. *J Sci Food Agric* **16**: 191–198 (1965).

19 Roig MG, Bello JF, Rivera ZS, Lloyd LL, Kennedy JF. Non-enzymatic browning in single-strength reconstituted citrus juice in tetrabrik cartons. *Biotechnol Prog* **12**: 281–285 (1996).

20 Kennedy JF, Rivera ZS, Lloyd LL, Warner FP, Jumel K. Studies on non-enzymic browning in orange juice using a model system based on freshly squeezed orange juice. *J Sci Food Agric* **52**: 85–95 (1990).

21 Stadtman ER. Nonenzymatic Browning in Fruit Products. *Adv Food Res* **1**: 325–372 (1948).

22 Buvé C, Kebede BT, De Batselier C, Carrillo C, Pham HTT, Hendrickx M *et al.* Kinetics of colour changes in pasteurised strawberry juice during storage. *J Food Eng* **216**: 42–51 (2018).

23 Paravisini L, Peterson DG. Role of Reactive Carbonyl Species in non-enzymatic browning of apple juice during storage. *Food Chem* **245**: 1010–1017 (2018).

24 Wibowo S, Grauwet T, Gedefa GB, Hendrickx M, Van Loey A. Quality changes of pasteurised mango juice during storage. Part II: Kinetic modelling of the shelf-life markers. *Food Res Int* **78**: 410–423 (2015).

25 Lee HS, Nagy S. Quality Changes and Nonenzymic Browning Intermediates in Grapefruit Juice During Storage. *J Food Sci* **53**: 168–172 (1988).

26 Clegg KM. Non-enzymic browning of lemon juice. *J Sci Food Agric* **15**: 878–885 (1964).

27 Solomon O, Svanberg U, Sahlström A. Effect of oxygen and fluorescent light on the quality of orange juice during storage at 8°C. *Food Chem* **53**: 363–368 (1995).

28 Polydera AC, Stoforos NG, Taoukis PS. Quality degradation kinetics of pasteurised and high pressure processed fresh Navel orange juice: Nutritional parameters and shelf life. *Innov Food Sci Emerg Technol* **6**: 1–9 (2005).

29 Wibowo S, Grauwet T, Santiago JS, Tomic J, Vervoort L, Hendrickx M *et al.* Quality changes of pasteurised orange juice during storage: A kinetic study of specific parameters and their relation to colour instability. *Food Chem* **187**: 140–151 (2015).

30 Vervoort L, Van Der Plancken I, Grauwet T, Timmermans RAH, Mastwijk HC, Matser AM *et al.* Comparing equivalent thermal, high pressure and pulsed electric field processes for mild pasteurization of orange juice: Part II: Impact on specific chemical and biochemical quality parameters. *Innov Food Sci Emerg Technol* **12**: 466–477 (2011).

31 Johnson JR, Braddock RJ, Chen CS. Kinetics of ascorbic-acid loss and nonenzymatic browning in orange juice serum-experimental rate constants. *J Food Sci* **60**: 502–505 (1995).

32 Koca N, Burdurlu HS, Karadeniz F. Kinetics of Nonenzymatic Browning Reaction in Citrus Juice

Concentrates during Storage. *Turkish J Agric For* **27**: 353–360 (2003).

33 Bull MK, Zerdin K, Howe E, Goicoechea D, Paramanandhan P, Stockman R *et al.* The effect of high pressure processing on the microbial, physical and chemical properties of Valencia and Navel orange juice. *Innov Food Sci Emerg Technol* **5**: 135–149 (2004).

34 Cortés C, Esteve MJ, Frígola A. Color of orange juice treated by High Intensity Pulsed Electric Fields during refrigerated storage and comparison with pasteurized juice. *Food Control* **19**: 151–158 (2008).

35 Lee HS, Chen CS. Rates of Vitamin C Loss and Discoloration in Clear Orange Juice Concentrate during Storage at Temperatures of 4−24 °C. *J Agric Food Chem* **46**: 4723–4727 (1998).

36 Nagy S, Lee H, Rouseff RL, Lin JCC. Nonenzymic Browning of Commercially Canned and Bottled Grapefruit Juice. *J Agric Food Chem* **39**: 9–13 (1990).

37 Polydera AC, Stoforos NG, Taoukis PS. Comparative shelf life study and vitamin C loss kinetics in pasteurised and high pressure processed reconstituted orange juice. *J Food Eng* **60**: 21–29 (2003).

38 Hsu HY, Tsai YC, Fu CC, Wu JSB. Degradation of ascorbic acid in ethanolic solutions. *J Agric Food Chem* **60**: 10696–10701 (2012).

Kennedy JF, Rivera ZS, Lloyd LL, Warner FP, Jumel K. l-Ascorbic acid stability in aseptically processed orange juice in TetraBrik cartons and the effect of oxygen. *Food Chem* **45**: 327–331 (1992).

40 Gómez Ruiz B, Roux S, Courtois F, Bonazzi C. Kinetic modelling of ascorbic and dehydroascorbic acids concentrations in a model solution at different temperatures and oxygen contents. *Food Res Int* **106**: 901–908 (2018).

41 Cao X, Bi X, Huang W, Wu J, Hu X, Liao X. Changes of quality of high hydrostatic pressure processed cloudy and clear strawberry juices during storage. *Innov Food Sci Emerg Technol* **16**: 181–190 (2012).

42 Robertson G, Samaniego C. Effect of initial dissolved oxygen levels on the de- gradation of ascorbic acid and the browning of lemon juice during storage. *J Food Sci* **51**: 184–187 (1986).

43 Arena E, Fallico B, Marracone E. Thermal damage in blood orange juice: kinetics of 5-hydroxymethyl-

2-furcarboxaldehyde formation. *Int J Food Sci Technol* **36**: 145–151 (2001).

44 Burdurlu HS, Koca N, Karadeniz F. Degradation of vitamin C in citrus juice concentrates during storage. *J Food Eng* **74**: 211–216 (2006).

45 Kanner J, Harel S, Fishbein Y, Shalom P. Furfural Accumulation in Stored Orange Juice Concentrates. *J Agric Food Chem* **29**: 948–949 (1981).

FIGURE LEGENDS

Figure 1. Schematic overview of the stepwise fractionation of orange juice.

Figure 2. Visual color changes during storage at 42 °C of plain orange juice, supernatant, 20 and 70% ethanol soluble material (ES20 and ES70, respectively), pellet fraction (pellet), and 20 and 70 % ethanol precipitated material (EP20 and EP70, respectively). (D: day(s), W: week(s)).

Figure 3. Changes in browning index (BI) during storage at 42 °C of the orange juice (◆), supernatant (■), 20% ethanol soluble material (▲), 70% ethanol soluble material (✕), pellet (●), 20% ethanol insoluble material (∗), and 70% ethanol insoluble material (+) fractions. The experimental data are represented by the different symbols and the full lines represent the fitted values by a first order fractional conversion model. The error bars indicate the standard deviation (sample size = 3).

Figure 4. Changes in different non-enzymatic browning-related attributes namely ascorbic acid content (A), dissolved oxygen content (B), headspace oxygen content (C), sucrose content (D), glucose content (E), fructose content (F), furfural content (G) and HMF content (H) during storage at 42 °C of the orange juice (◆), supernatant (■), 20% ethanol soluble material (▲), and 70% ethanol soluble material (✕). The experimental data are represented by the different symbols and the full lines represent the fitted values by zero order (glucose, fructose, furfural), first order (ascorbic acid, sucrose), first order fractional conversion (dissolved and headspace oxygen), and logistic (HMF) models. The error bars indicate the standard deviation (sample size = 3).

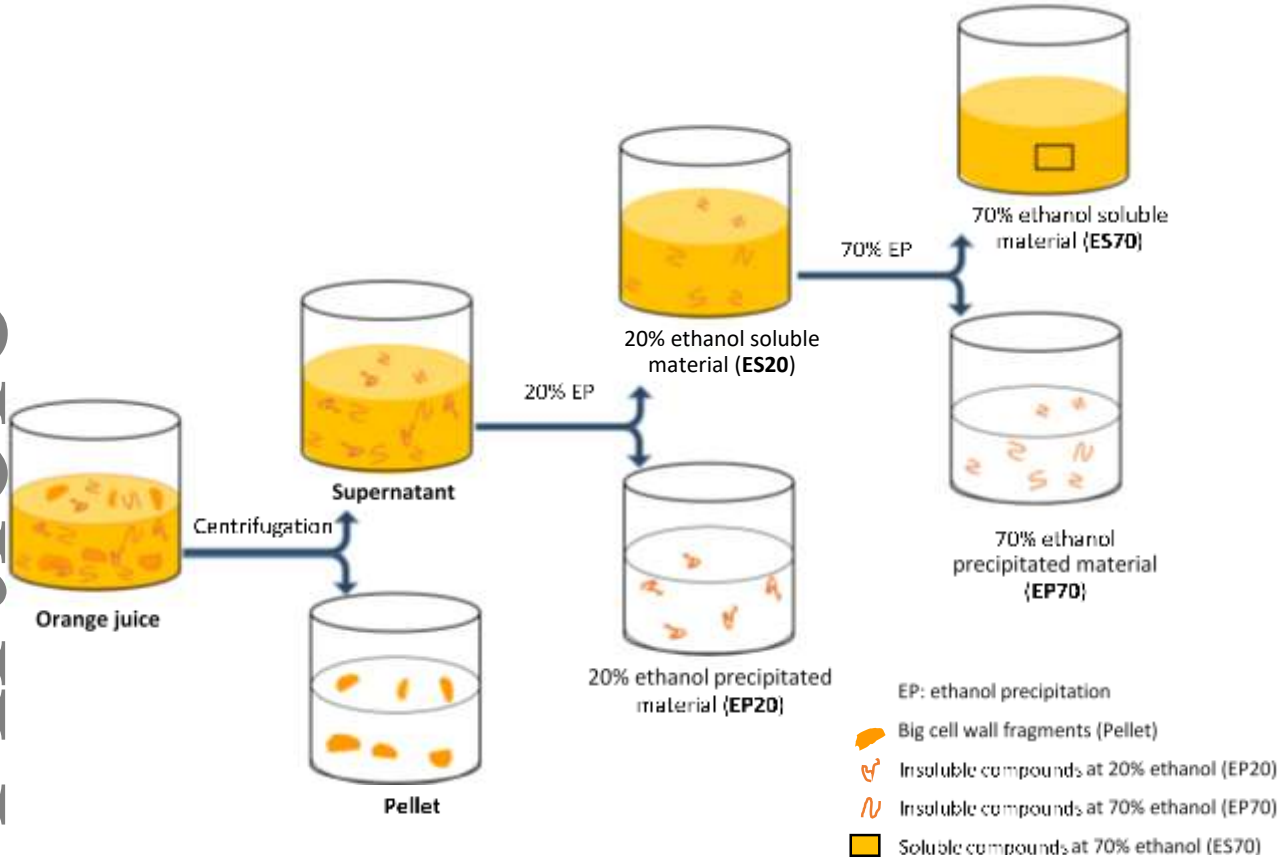

Figure 1. Schematic overview of the stepwise fractionation of orange juice.

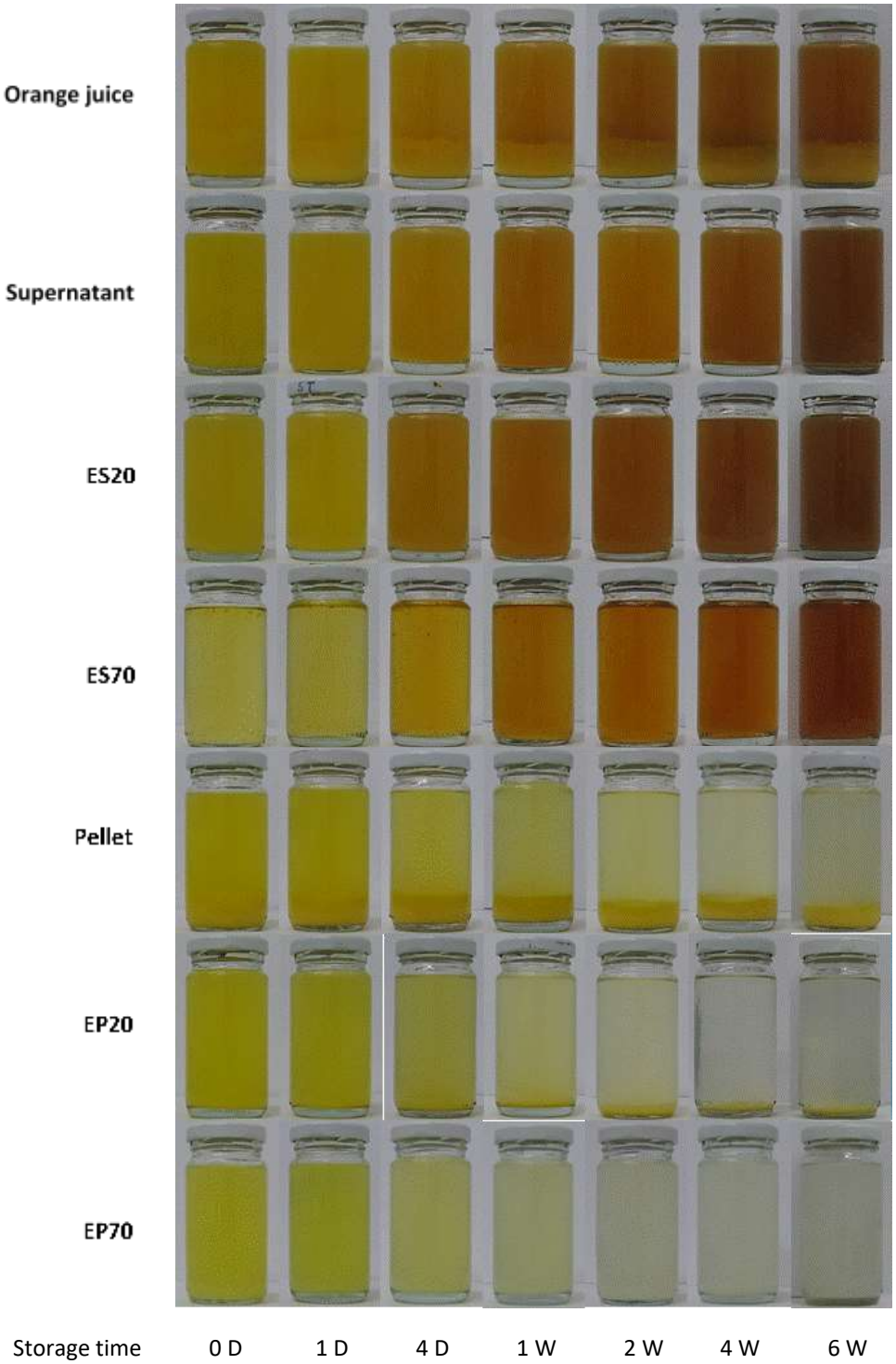

Figure 2. Visual color changes during storage at 42 °C of plain orange juice, supernatant, 20 and 70% ethanol soluble material (ES20 and ES70, respectively), pellet fraction (pellet), and 20 and 70 % ethanol precipitated material (EP20 and EP70, respectively). (D: day(s), W: week(s)).

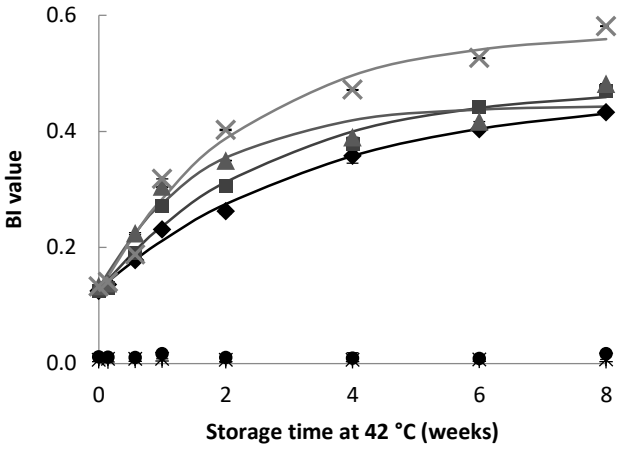

Figure 3. Changes in browning index (BI) during storage at 42 °C of the orange juice (◆), supernatant (■), 20% ethanol soluble material (▲), 70% ethanol soluble material (×), pellet (●), 20% ethanol insoluble material (∗), and 70% ethanol insoluble material (+) fractions. The experimental data are represented by the different symbols and the full lines represent the fitted values by a first order fractional conversion model. The error bars indicate the standard deviation (sample size = 3).

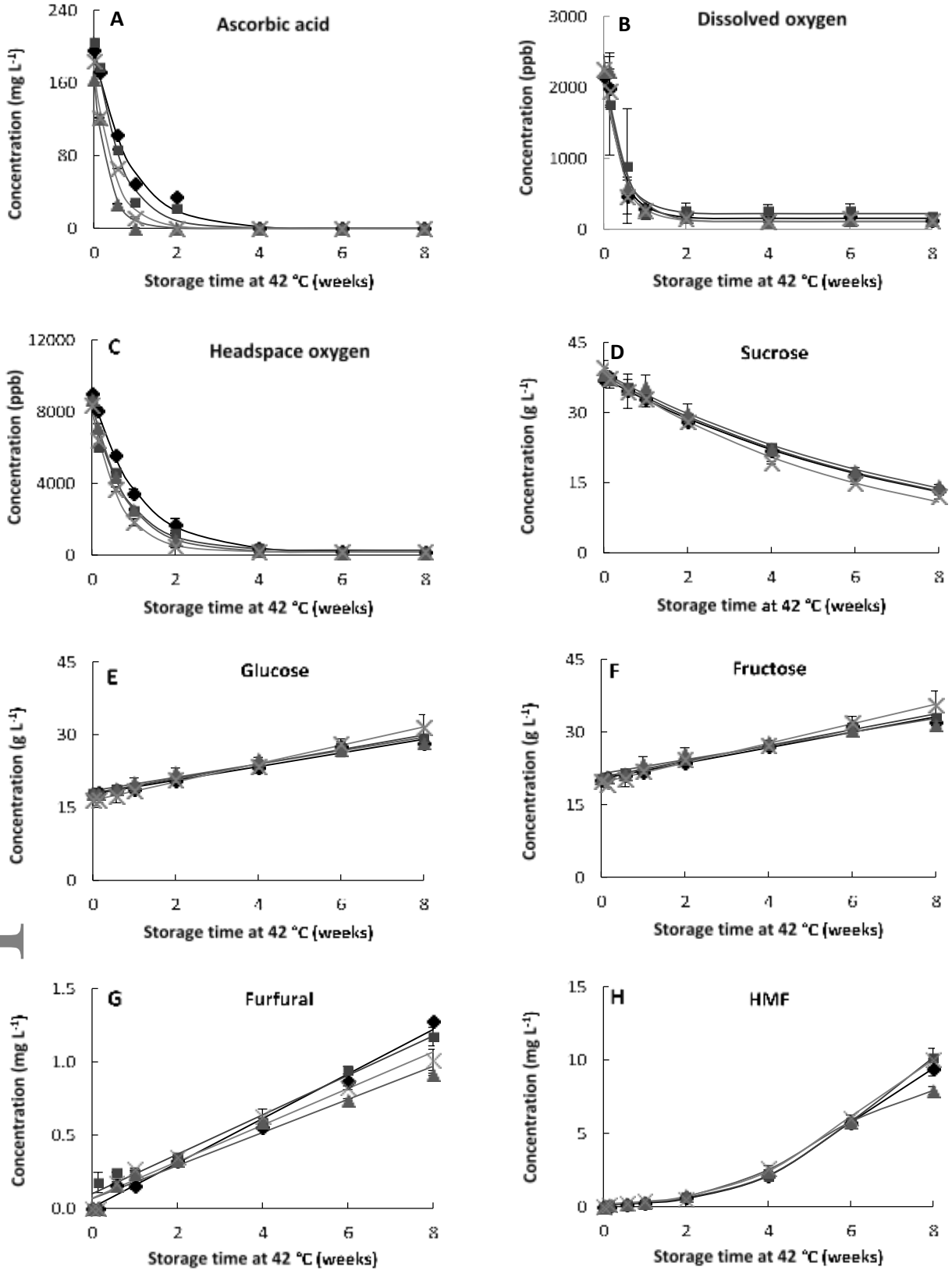

Figure 4. Changes in different non-enzymatic browning related attributes namely ascorbic acid content (A), dissolved oxygen content (B), headspace oxygen content (C), sucrose content (D), glucose content (E), fructose content (F), furfural content (G) and HMF content (H) during storage at 42 °C of the orange juice (◆), supernatant (■), 20% ethanol soluble material (▲), and 70% ethanol soluble material (✕). The experimental data are represented by the different symbols and the full lines represent the fitted values by zero order (glucose, fructose, furfural), first order (ascorbic acid, sucrose), first order fractional conversion (dissolved and headspace oxygen), and logistic (HMF) models. The error bars indicate the standard deviation (sample size = 3).

Table 1. Estimated parameters (± standard error) based on a first order fractional conversion (for browning index (BI), dissolved oxygen and headspace oxygen), first order (for ascorbic acid (AA) and sucrose), zero order (for glucose, fructose, and furfural), and logistic (5-hydroxymethyl furfural (HMF)) kinetic model describing changes during storage at 42 °C of the orange juice, supernatant, 20% ethanol soluble material (ES20), and 70% ethanol soluble material (ES70).

Sample	*BI (First order fractional conversion model)*				*AA degradation (First order model)*			*Fructose formation (Zero order model)*		
	X_o	X_∞	k (week^{-1})	R^2_{adj}	X_o (mg L^{-1})	k (week^{-1})	R^2_{adj}	X_o (g L^{-1})	k (g L^{-1} week^{-1})	R^2_{adj}
Orange juice	0.128 ± 0.007^{a}	0.465 ± 0.020^{a}	0.287 ± 0.042^{a}	0.99	197.5 ± 6.8^{ab}	1.17 ± 0.10^{a}	0.99	20.35 ± 0.35^{ab}	1.59 ± 0.09^{a}	0.98
Supernatant	0.125 ± 0.014^{a}	0.476 ± 0.025^{a}	0.383 ± 0.080^{a}	0.98	210.8 ± 7.6^{b}	1.60 ± 0.15^{ab}	0.99	20.67 ± 0.20^{b}	1.63 ± 0.05^{a}	0.99
ES20	0.129 ± 0.021^{a}	0.445 ± 0.021^{a}	0.627 ± 0.154^{a}	0.96	169.3 ± 5.6^{a}	2.96 ± 0.27^{c}	0.99	21.36 ± 0.53^{ab}	1.43 ± 0.13^{a}	0.95
ES70	0.121 ± 0.021^{a}	0.572 ± 0.029^{a}	0.448 ± 0.093^{a}	0.98	179.0 ± 7.3^{ab}	2.15 ± 0.23^{bc}	0.99	19.56 ± 0.24^{a}	2.02 ± 0.06^{b}	0.99

For each attribute listed in the same column, estimates which are significantly different between samples are indicated with a different letter in superscript ($p < 0.05$).

Sample	*Dissolved oxygen consumption (First order fractional conversion model)*				*Sucrose degradation (First order model)*			*Furfural formation (Zero order model)*		
	X_o (ppb)	X_∞ (ppb)	k (week^{-1})	R^2_{adj}	X_o (g L^{-1})	k (week^{-1})	R^2_{adj}	X_o (mg L^{-1})	k (mg L^{-1} week^{-1})	R^2_{adj}
Orange juice	2321 ± 167^{a}	153 ± 91^{a}	2.50 ± 0.58^{a}	0.96	37.41 ± 0.30^{a}	0.132 ± 0.004^{a}	0.99	0.005 ± 0.025^{a}	0.152 ± 0.006^{b}	0.99
Supernatant	2436 ± 269^{a}	222 ± 63^{a}	2.48 ± 0.54^{a}	0.96	37.96 ± 0.19^{a}	0.132 ± 0.002^{a}	0.99	0.100 ± 0.030^{a}	0.134 ± 0.008^{ab}	0.98
ES20	2459 ± 201^{a}	108 ± 114^{a}	2.18 ± 0.56^{a}	0.95	38.47 ± 0.49^{a}	0.128 ± 0.006^{a}	0.99	0.066 ± 0.032^{a}	0.113 ± 0.008^{a}	0.97
ES70	2386 ± 136^{a}	115 ± 74^{a}	2.58 ± 0.47^{a}	0.98	38.47 ± 0.50^{a}	0.158 ± 0.007^{b}	0.99	0.068 ± 0.033^{a}	0.125 ± 0.008^{ab}	0.97
Sample	*Headspace oxygen consumption (First order fractional conversion model)*				*Glucose formation (Zero order model)*			*HMF formation (Logistics model)*		
	X_o (ppb)	X_∞ (ppb)	k (week^{-1})	R^2_{adj}	X_o (g L^{-1})	k (g L^{-1} week^{-1})	R^2_{adj}	λ (week)	X_∞ (mg L^{-1})	k (mg L^{-1} week^{-1})	R^2_{adj}
Orange juice	9084 ± 117^{b}	196 ± 92^{a}	0.93 ± 0.04^{a}	0.99	17.77 ± 0.33^{b}	1.41 ± 0.08^{a}	0.98	3.34 ± 0.07^{b}	11.54 ± 0.36^{b}	2.15 ± 0.05^{b}	0.99
Supernatant	8077 ± 410^{ab}	278 ± 289^{a}	1.18 ± 0.19^{ab}	0.98	18.95 ± 0.16^{b}	1.50 ± 0.04^{a}	0.99	3.54 ± 0.06^{b}	13.47 ± 0.50^{b}	2.35 ± 0.04^{b}	0.99
ES20	8610 ± 69^{ab}	162 ± 47^{a}	1.25 ± 0.03^{b}	0.99	18.43 ± 0.41^{b}	1.38 ± 0.11^{b}	0.97	2.62 ± 0.07^{a}	8.76 ± 0.19^{a}	1.72 ± 0.05^{a}	0.99
ES70	8249 ± 123^{a}	176 ± 78^{a}	1.56 ± 0.07^{b}	0.99	16.45 ± 0.17^{a}	1.89 ± 0.04^{b}	0.99	3.20 ± 0.11^{b}	12.65 ± 0.68^{b}	2.19 ± 0.07^{b}	0.99